EUROPEAN ORGANIZATION FOR NUCLEAR RESEARCH (CERN)

September 2015

Feasibility study on using $\phi \to K^0\overline{K}^0$ at LHCb to test for CPT invariance

Sonja Verena Bartkowski
Supervisors: Giulio Dujany & George Lafferty

Abstract

The quantum mechanical system $\phi \to K^0\overline{K}^0$ offers the means for studying CPT invariance. If CPT is violated intrinsically, for example if the CPT operator itself is not well defined, it becomes apparent in quantum decoherence within the considered system. This report summarizes a CERN summer student project that looked at the feasibility of such a study in LHC proton-proton collisions at the LHCb detector.

© CERN on behalf of the LHCb collaboration, licence CC-BY-4.0.

1 CPT invariance

The Standard Model of Particle Physics builds on the assumption of invariance under CPT transformation, i.e. the invariance under combined charge conjugation (C), parity inversion (P), and time inversion (T). As the CPT theorem states, this invariance is given for any quantum theory formulated on flat space-times, provided the theory respects (i) Locality, (ii) Unitarity (i.e. conservation of probability), and (iii) Lorentz invariance [1], [2].

With the system $\phi \to K^0\overline{K}^0$, the aspect of unitarity, which - if not given - allows for CPT violation within quantum mechanics, can be probed.

2 The system studied

Since the strong decay $\phi \to K^0\overline{K}^0$ conserves angular momentum and CP eigenvalues, the two kaons form an antisymmetric state which can be written as

$$|\phi\rangle \to \frac{1}{\sqrt{2}}\left(\left|K^0\overline{K}^0\right\rangle - \left|\overline{K}^0K^0\right\rangle\right) = \frac{\mathcal{N}}{\sqrt{2}}\left(|K_SK_L\rangle - |K_LK_S\rangle\right) \tag{1}$$

where $\mathcal{N} = \frac{1+|\epsilon|^2}{1-\epsilon^2}$ and $|K_S\rangle = \frac{1}{\sqrt{1+|\epsilon|^2}}\left(|K_+\rangle + \epsilon\,|K_-\rangle\right)$ as well as $|K_L\rangle = \frac{1}{\sqrt{1+|\epsilon|^2}}\left(|K_+\rangle + \epsilon\,|K_-\rangle\right)$. The states $|K^0\rangle$ and $|\overline{K}^0\rangle$ are flavor eigenstates, $|K_S\rangle$ and $|K_L\rangle$ are mass eigenstates in which the kaons propagate, and $|K_+\rangle$ and $|K_-\rangle$ are CP eigenstates. Because the mass eigenstates and the CP eigenstates are not equivalent, CP is violated, i.e. both K_S and K_L can decay into two charged pions with $\mathcal{B}(K_S \to \pi^+\pi^-) = (69.20 \pm 0.05)\%$ and $\mathcal{B}(K_L \to \pi^+\pi^-) = (1.967 \pm 0.010) \cdot 10^{-3}$ respectively [3]. These two decays lead to an interference term in the decay intensity

$$I(t_1, t_2) \propto e^{-\Gamma_L t_1 - \Gamma_S t_2} + e^{-\Gamma_S t_1 - \Gamma_L t_2} - 2e^{-\frac{1}{2}(\Gamma_S+\Gamma_L)(t_1+t_2)}\cos\left(\Delta m\,(t_1 - t_2)\right) \tag{2}$$

where $t_{1,2}$ are the decay times of the two kaons, $\Gamma_{S,L}$ are the decay widths of K_S and K_L, and $\Delta m = |m_{K_L} - m_{K_S}|$ is the mass difference between them. The effects of a non-unitary time evolution due to CPT violation can be parameterized by introducing a decoherence term ζ_{SL} [4].

$$I(t_1, t_2) \propto e^{-\Gamma_L t_1 - \Gamma_S t_2} + e^{-\Gamma_S t_1 - \Gamma_L t_2} - 2(1-\zeta_{SL})e^{-\frac{1}{2}(\Gamma_S+\Gamma_L)(t_1+t_2)}\cos\left(\Delta m\,(t_1 - t_2)\right). \tag{3}$$

Though there are many different models that describe CPT violation, this study will only consider this one.

If ζ_{SL} is non-zero, this manifests itself in an excess of decays with small decay time differences $\Delta t = |t_1 - t_2|$ as shown in figure 1.

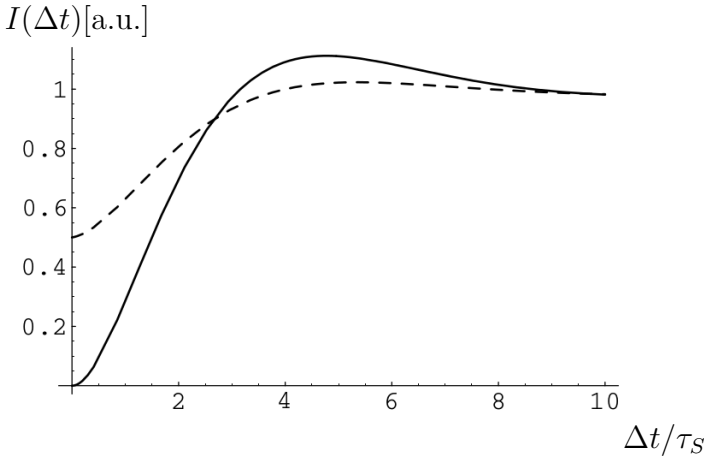

Figure 1: Decay intensity $I(\Delta t)$ of $\phi \to \pi^+\pi^-\pi^+\pi^-$. The solid line is for $\zeta_{SL} = 0$ and the dashed line for $\zeta_{SL} \neq 0$. [2]

The currently best 95% C.L. limit on this parameter is set by KLOE with $\zeta_{SL} = 0.098$ [5].

2.1 ϕ Production channels

At LHCb, two ϕ production channels can be taken into consideration to do this study. One uses prompt ϕ coming directly from the primary vertex and the other uses ϕ from the decay $D_s^\pm \to \phi\pi^\pm$. Both production channels are illustrated in figure 2.

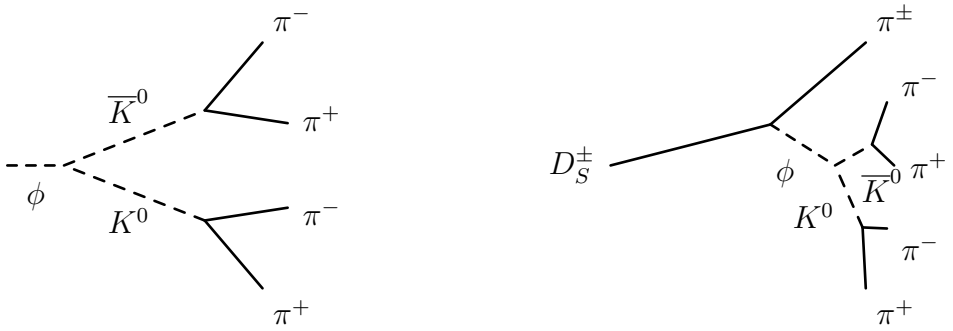

Figure 2: Topology of prompt ϕ production (left) and $D_s^\pm \to \phi\pi^\pm$ (right) and the decay $\phi \to K^0\overline{K}^0 \to \pi^+\pi^-\pi^+\pi^-$. Solid lines indicate charged particles with tracks, dashed lines indicate neutral particles.

Including a cut on LHCb's geometric acceptance, the production cross sections for 14 TeV as extrapolated from the 7 TeV cross sections are for prompt ϕ 3516 µb [6] and for $D_s^\pm$ 388 µb [7]. Additionally, the branching fraction $\mathcal{B}(D_s^\pm \to \phi\pi^\pm) = (4.5 \pm 0.4)\%$ has to be taken into account for the production rate of ϕ in the $D_s^\pm$ channel. Both approaches are considered because the production rate of prompt ϕ is considerably higher than that of ϕ from $D_s^\pm$ decays, but $D_s^\pm \to \phi\pi^\pm$ might offer a better handle on background rejection because of the displaced $D_s^\pm$ vertex and a constraint on the $D_s^\pm$ mass.

2.2 Background processes

If one considers the excess of $\phi \to K^0\overline{K}^0 \to \pi^+\pi^-\pi^+\pi^-$ for small Δt due to CPT violation as signal, there are three main sources of background. One is the decay mode $\phi \to K_L K_S \to \pi^+\pi^-\pi^+\pi^-$ resulting from CP violation which from here one is going to be referred to as Standard Model (SM) background. Its decay intensity is plotted as the solid line in figure 1. The second background is so called regeneration background which results from the interaction of K_L with matter and causes a transformation $K_L \to K_S$. The third background is combinatoric background of prompt kaons and pions.

2.3 Track types

In LHCb, different track types are defined depending on the sub-detectors in which the hits used to reconstruct the track are located. A schematic overview of the track types is given in figure 3. For this study, we will consider only long tracks which are reconstructed with hits in the VELO and the other components of the tracking system, and downstream tracks which do not have hits in the VELO. Depending on its decay time a kaon can decay inside or outside the VELO and thus be reconstructed using two long pion tracks (LL) or two downstream pion tracks (DD). Kaons with long decay times are reconstructed using downstream tracks and kaons with short decay times are reconstructed using long tracks.

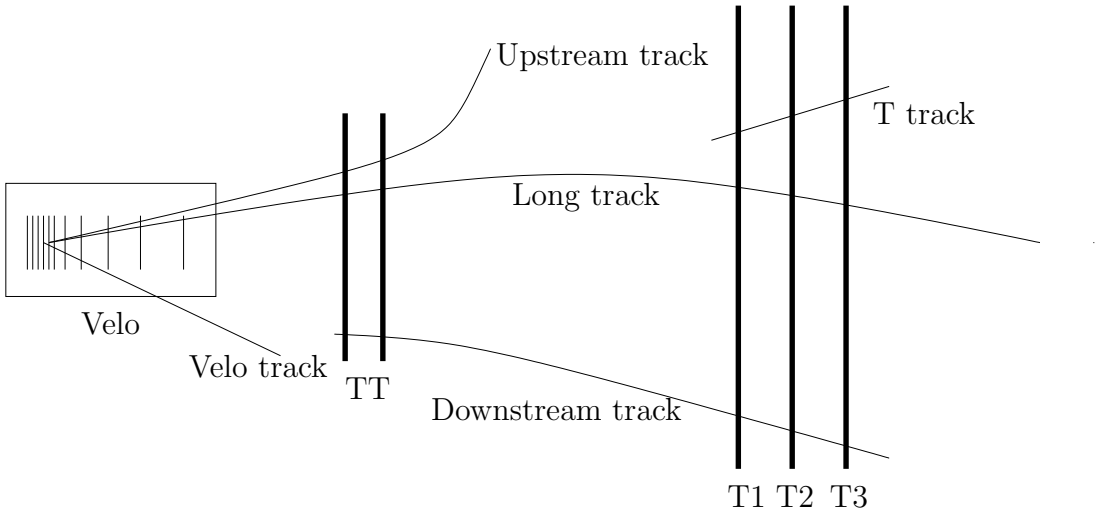

Figure 3: Track types in LHCb: Upstream tracks are in the VELO and TT, downstream tracks in both outer trackers, and long tracks in all trackers. [8]

3 Detector and processing efficiencies

3.1 Dataset and selection

To determine the number of events expected both for signal and background processes, Monte Carlo samples of prompt ϕ and $D_s^\pm \to \phi\pi^\pm$ have been used. These Monte Carlo

files contain $1 \cdot 10^4$ events each.
For the selection the stripping line `PhiToKSKS` has been used. The version used in this study is not the final one. It can be found at `https://github.com/gdujany/phi2KsKs/blob/master/StrippingPhiToKSKS.py`.
A summary of the cuts in the stripping line are given in table 1.

	Prompt ϕ	$D_s^\pm \to \phi\pi^\pm$
π from LL K_S	TRGHOSTPROB < 0.35 P $> 2\,$GeV MIPCHI2DV(PRIMARY) > 9	TRGHOSTPROB < 0.35 P $> 2\,$GeV MIPCHI2DV(PRIMARY) > 9
π from DD K_S	P $> 2\,$GeV MIPCHI2DV(PRIMARY) > 4	P $> 2\,$GeV MIPCHI2DV(PRIMARY) > 4
K_S	ADOCACHI2CUT(25, '') VFASPF(VCHI2) < 25 PT $> 500\,$MeV ADMASS('KS0') $< 20\,$MeV BPVVD $> 10\,$mm BPVVDCHI2 > 50 VFASPF(VCHI2PDOF) < 10 BPVDIRA > 0.9999	ADOCACHI2CUT(25, '') VFASPF(VCHI2) < 25 PT $> 500\,$MeV ADMASS('KS0') $< 20\,$MeV BPVVD $> 10\,$mm BPVVDCHI2 > 50 VFASPF(VCHI2PDOF) < 10 BPVDIRA > 0.9999
ϕ	LL LL or LL DD combinations APT $> 1000\,$MeV AM $< 1100\,$MeV ACUTDOCACHI2(100,'') M $< 1070\,$MeV VFASPF(VCHI2/VDOF) < 10 MIPCHI2DV(PRIMARY) < 100	LL LL or LL DD combinations APT $> 1000\,$MeV AM $< 1100\,$MeV ACUTDOCACHI2(100,'') M $< 1090\,$MeV VFASPF(VCHI2/VDOF) < 10 MIPCHI2DV(PRIMARY) < 100
π from D_s		PT $> 250\,$MeV MIPCHI2DV(PRIMARY) > 4 MIPCHI2DV(PRIMARY) < 300 TRGHOSTPROB < 0.35
D_s		APT $> 800\,$MeV ADAMASS(1920 MeV) $< 130\,$MeV ACUTDOCACHI2(100,'') DMASS(1920 MeV) $< 100\,$MeV VFASPF(VCHI2/VDOF) < 10 MIPCHI2DV(PRIMARY) < 100
Post-stripping cuts	1010 MeV <phi_M< 1030 MeV	1010 MeV <phi_M< 1030 MeV 1955 MeV<Ds_M<1985 MeV IPCHI2 ≥ 15

Table 1: Summary of all cuts done in the stripping line and in post-stripping selection, both for prompt ϕ and $D_s^\pm \to \phi\pi^\pm$.

The mass windows used for all following studies are $1010\,\text{MeV} < m(\phi) < 1030\,\text{MeV}$ and $1955\,\text{MeV} < m(D_s^\pm) < 1985\,\text{MeV}$. In order to reject prompt ϕ, in the $D_s^\pm \to \phi\pi^\pm$ selection

the cut $\chi^2 \geq 15$ on the χ^2 of a fit matching the ϕ origin vertex to the primary vertex was added.

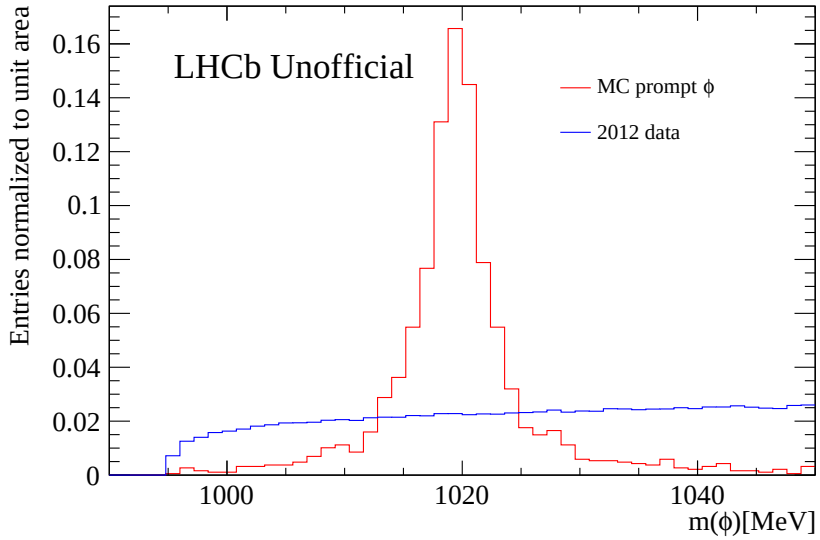

Figure 4: Invariant mass of ϕ after applying the selection. The Monte Carlo shows the spectrum for $\phi \to K_S K_S \to \pi^+\pi^-\pi^+\pi^-$ whereas the 2012 data contains mostly background events.

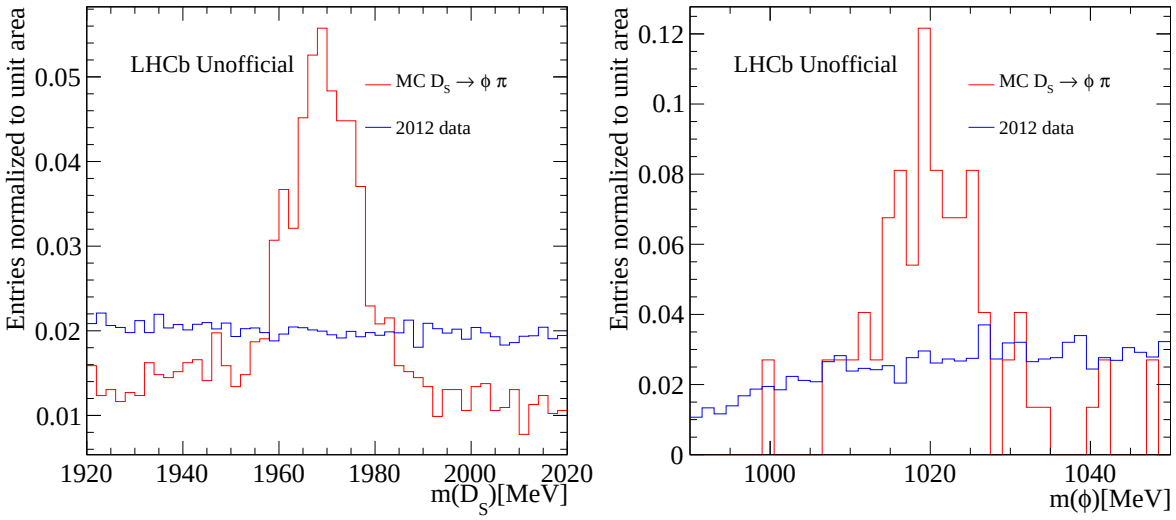

Figure 5: Invariant mass of D_s and ϕ after applying the selection. The Monte Carlo shows the spectra for $D_s^{\pm} \to \phi\pi^{\pm} \to K_S K_S \to \pi^+\pi^-\pi^+\pi^-\pi^{\pm}$ whereas the 2012 data contains mostly background events.

Additional to the signal Monte Carlo samples, the 2012 data set was processed with the selection. For the prompt ϕ selection, the `CHARM.mDST` container was used, as was the

`CHARMCOMPLETEEVENT.DST` container for the $D_s^{\pm} \to \phi\pi^{\pm}$ selection (both are `Reco14`). The resulting spectra of the invariant masses of ϕ and $D_s^{\pm}$ normalized to unit area can be found in figures 4 and 5.

3.2 Efficiencies

From the Monte Carlo, reconstruction and trigger efficiencies have been determined. The probabilities of the kaon decays have been determined using the decay intensities in equation (2) and (3), with ζ_{SL} set to 0.098, the 95% C.L. limit set by KLOE. It is estimated that to decay, on average, inside the beampipe, the decay time of the kaons has to be less than 25 ps, and to be reconstructed at all, the decay time has to be less than 200 ps. The estimate for the background yield is the number of events in the 2012 data after applying the selection. All resulting values can be found in table 2.

	Prompt ϕ	$D_s \to \phi\pi$
Cross section (14 TeV), LHCb acceptance	3516 µb	388 µb
Branching fractions	34.2%	4.5% · 34.2%
Fiducial cuts efficiency	2.5%	7.0%
Probability $K_sK_s \to 4\pi$, exactly 1 (2) decays inside beampipe	15.1% (2.8%)	
Probability $K_sK_L \to 4\pi$ (CPV), exactly 1 (2) decays inside beampipe	$3.98 \cdot 10^{-7}$ ($4.99 \cdot 10^{-10}$)	
Upper limit KLOE probability $K_sK_L \to 4\pi$ (CPV + CPTV), exactly 1 (2) decays inside beampipe	$5.13 \cdot 10^{-7}$ ($1.64 \cdot 10^{-8}$)	
Reconstruction & selection efficiency	7.9% (7.6%)	1.4% (3.9%)
L0 efficiency	16.1% (18.6%)	23.0% (19.5%)
HLT1 efficiency	13.7% (16.7%)	35.6% (25.0%)
HLT2 efficiency	65.6% (100.0%)	68.8% (100.0%)
Total efficiency	$4.39 \cdot 10^{-5}$ ($5.85 \cdot 10^{-5}$)	$8.18 \cdot 10^{-5}$ ($1.32 \cdot 10^{-4}$)
Expected events SM background / fb^{-1}	21 ($3.51 \cdot 10^{-2}$)	$1.94 \cdot 10^{-1}$ ($3.94 \cdot 10^{-4}$)
Upper limit for SM background + signal (KLOE) / fb^{-1}	27 (1.15)	$2.5 \cdot 10^{-1}$ ($1.29 \cdot 10^{-2}$)
Combinatoric background (data 2012) / fb^{-1}	163110 (29120)	450 (2030)

Table 2: Cross sections, branching fractions, efficiencies and resulting event yields for signal, standard model background, and combinatoric background. If two numbers are given, the one in brackets assumes two kaons decaying inside the beampipe, whereas for the other it is required that exactly one of the two kaons decays inside the beampipe.

From the event yield one can conclude that the signal to background ratio is in the same order of magnitude for both approaches and not much is gained from using the $D_s^{\pm} \to \phi\pi^{\pm}$ approach.

4 Background studies with minimum bias Monte Carlo

In order to better understand the combinatoric background, minimum bias Monte Carlo files[1] have been processes with the same selections as described in section 3. From the 42 million input events, those that remain after the selection have the following background categories:

Background category	Prompt ϕ	$D_s \to \phi\pi$
light flavour	17(17)	0
$b\bar{b}$	1(1)	0
different PV	3(2)	0
physical bkg, partl. reconstructed	1(1)	1(1)
ghosts	0	1(0)
total	21(20)	2(1)

Table 3: Background categories of the minimum bias Monte Carlo events remaining after the selection. The number in brackets is the number of background events with true K_S.

It can be concluded that 80% of the background after the prompt ϕ selection is prompt K_S originating from the primary vertex. For the $D_s^{\pm} \to \phi\pi^{\pm}$ selection, the number of events in the Monte Carlo sample is too low to gain more information about the background types.

5 Time resolution

Since CPT violation would be visible as an excess of $\phi \to K^0\overline{K}^0 \to \pi^+\pi^-\pi^+\pi^-$ for small Δt, knowledge about the time resolution of the detector for this system is important. Two differenent methods have been considered for the reconstruction of the decay times. The first uses the DaVinci class TupleToolPropertime to determine the decay times from the reconstructed particles. The standard reconstruction follows a bottom-up approach, starting with parameters of the reconstructed final state particles and then working its way up by determining the parameters of each mother particle via a fit to those parameters of its daughter particles [9]. The second method uses the DecayTreeFitter which performs a simultaneous fit of all vertices [9]. For this study, in this fit, the kaon mass was constrained to the nominal K_S mass.

[1]The files can be found in the LHCb bookkeeping under the references `/MC/2012/30000000/Beam4000GeV-2012-MagUp-Nu2.5-Pythia8/Sim08a/Digi13/Trig0x409f0045/Reco14a/Stripping20NoPrescalingFlagged/ALLSTREAMS.DST`, `/MC/2012/30000000/Beam4000GeV-2012-MagDown-Nu2.5-Pythia8/Sim08a/Digi13/Trig0x409f0045/Reco14a/Stripping20NoPrescalingFlagged/ALLSTREAMS.DST`, `/MC/2012/30000000/Beam4000GeV-2012-MagUp-Nu2.5-Pythia8/Sim08c/Digi13/Trig0x409f0045/Reco14a/Stripping20NoPrescalingFlagged/ALLSTREAMS.DST`, and `/MC/2012/30000000/Beam4000GeV-2012-MagDown-Nu2.5-Pythia8/Sim08c/Digi13/Trig0x409f0045/Reco14a/Stripping20NoPrescalingFlagged/ALLSTREAMS.DST`.

To determine the resolution, the reconstructed decay times t(reconstructed) were compared with the true decay times t(true) for the $D_S^{\pm} \to \phi\pi^{\pm}$ and the prompt ϕ Monte Carlo, the different figures being presented next to each other in the following.

5.1 Using the DecayTreeFitter

The DecayTreeFitter does not allow for negative decay times. Therefore

$$t(\text{reconstructed}) - t(\text{true}) \geq -t(\text{true}), \tag{4}$$

which leads to a sharp edge for negative residuals as illustrated for LL kaons in figure 6. The resolution was estimated by fitting the residual for those cases where t(reconstructed)$-$ t(true) ≥ 0 to a Breit Wigner distribution

$$N(\delta t) = \frac{a}{(\delta t - \mu)^2 - \Gamma^2/4}, \qquad \delta t = t(\text{reconstructed}) - t(\text{true}) \tag{5}$$

as shown in figure 7. For this specific fit, the centre was fixed to $\mu = 0$.

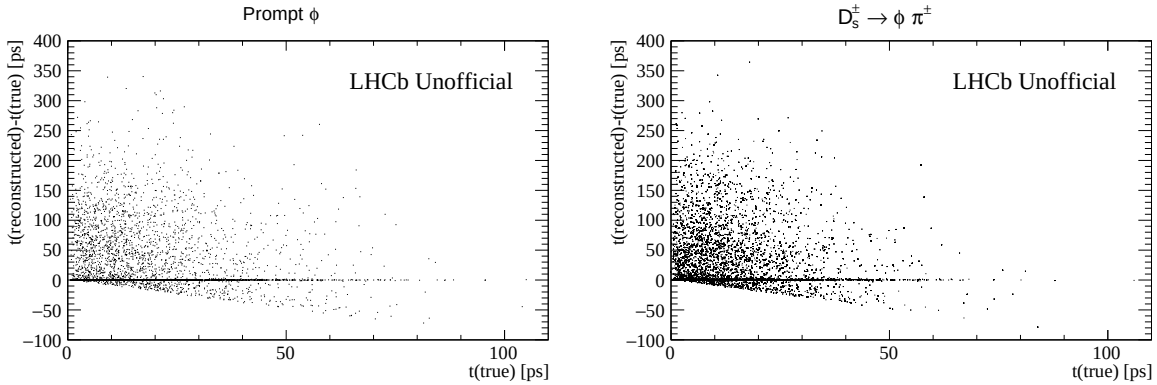

Figure 6: Residual of t for LL kaons reconstructed via DecayTreeFitter plotted against the true value of t.

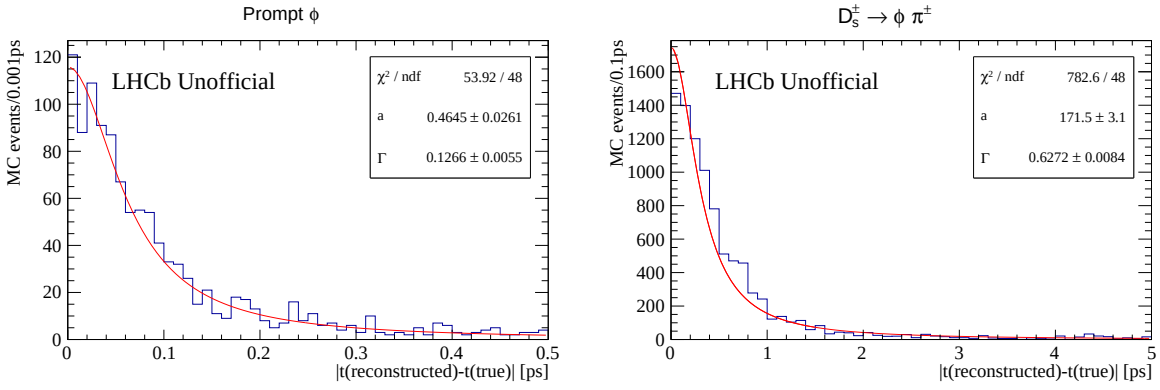

Figure 7: Resolution of LL kaon decay times t reconstructed via the DecayTreeFitter.

For DD kaons, sensitivity on the decay times is not given because the DecayTreeFitter sometimes reconstructs the decay times of the kaons as close to zero, maybe due to a lack of information available, which can be seen in figure 8. This results in an underestimation of the decay times as shown in figure 9.

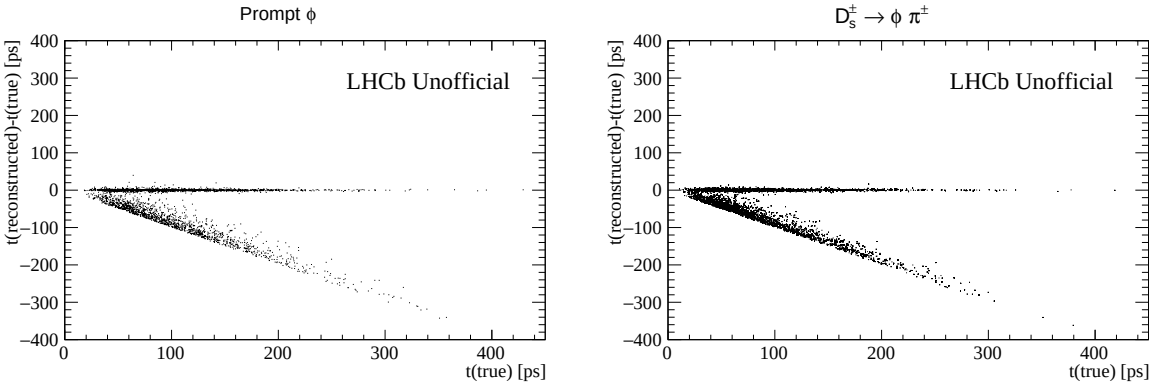

Figure 8: Residual of t for DD kaons reconstructed via DecayTreeFitter plotted against the true value of t.

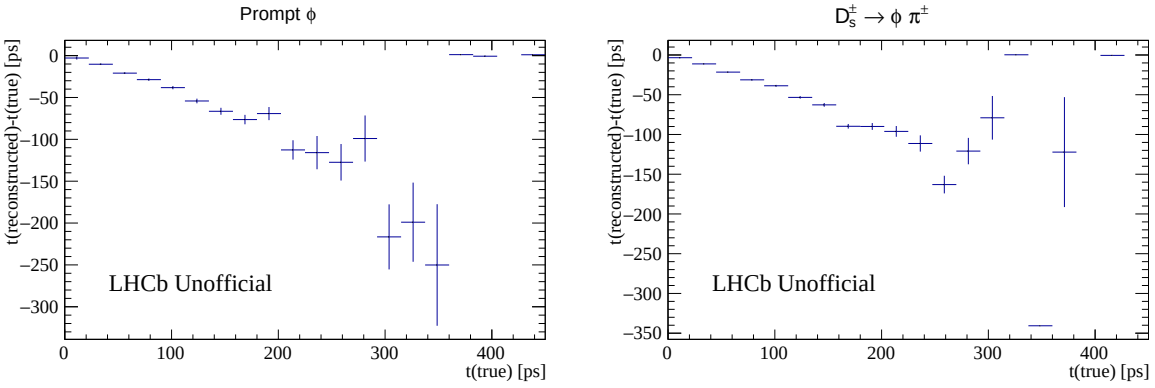

Figure 9: Average residual of t for DD kaons reconstructed via DecayTreeFitter plotted against the true value of t.

Therefore it is not advised to use the DecayTreeFitter in the context of decay time reconstruction with downstream tracks.
Since for probing the CPT invariance of the system, the observable $\Delta t = |t_1 - t_2|$ is used, its resolution for LL kaons has been studied as well, as it is displayed in figure 10. To do this, the residual $\delta(\Delta t)$ has been fitted to the Breit Wigner distribution

$$N(\delta(\Delta t)) = \frac{a}{(\delta(\Delta t) - \mu)^2 - \Gamma^2/4}. \tag{6}$$

All resolution widths for LL kaons are given in table 4.

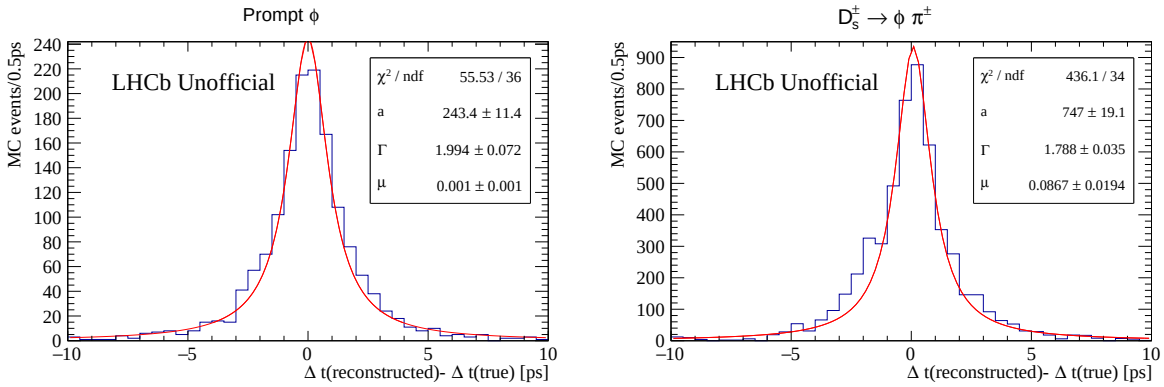

Figure 10: Resolution of Δt reconstructed via DecayTreeFitter LL kaons.

Distribution	Prompt ϕ	$D_s^{\pm} \to \phi\pi^{\pm}$
t	0.127 ± 0.006	0.627 ± 0.008
Δt	1.99 ± 0.07	1.79 ± 0.04

Table 4: Width Γ [ps] of the given distributions of decay times and decay time differences for LL kaons reconstructed via the DecayTreeFitter.

5.2 Using the TupleToolPropertime

The TupleToolPropertime does not explicitly exclude negative decay times. Therefore, the difference between reconstructed and true decay time relative to the true decay time is symmetric as seen in figures 11 and 12. The average residual of the decay time in figure 13 confirms this.

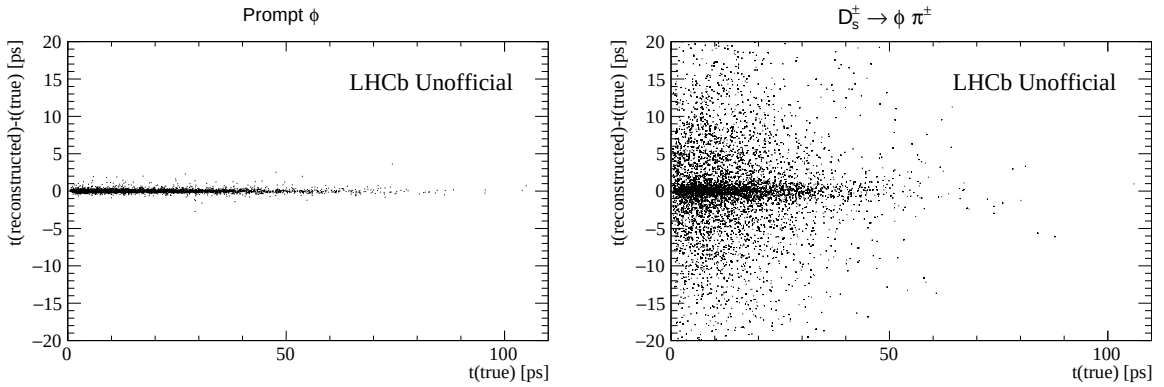

Figure 11: Residual of t for LL kaons reconstructed using the TupleToolPropertime plotted against the true value of t.

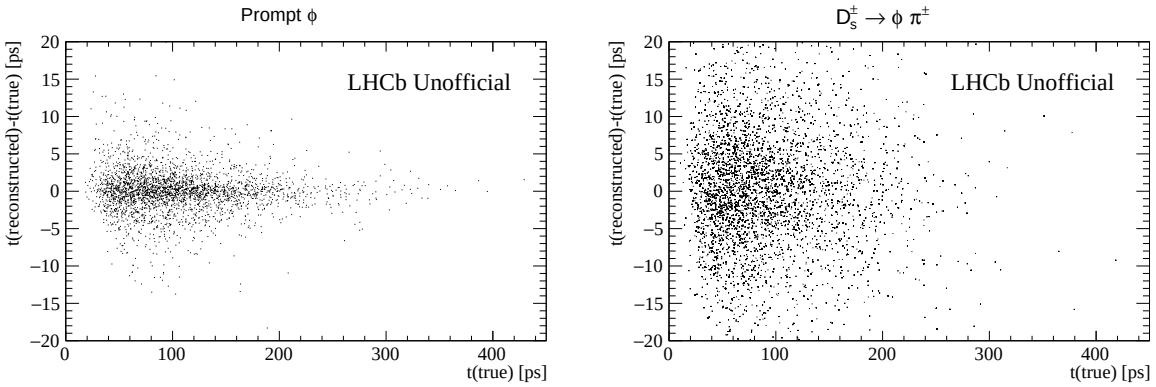

Figure 12: Residual of t for DD kaons reconstructed using TupleToolPropertime plotted against the true value of t.

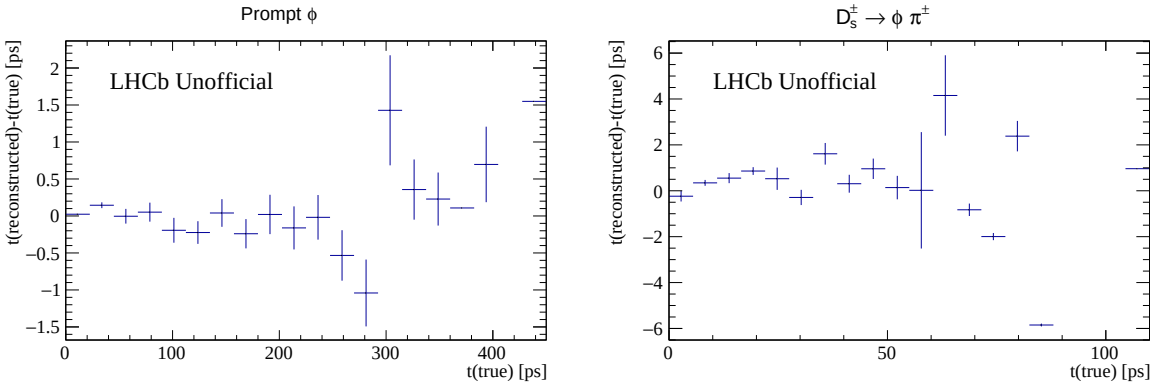

Figure 13: Average of t reconstructed using TupleToolPropertime for all kaons plotted against the true value of t.

The decay time resolution has been fitted to the Breit Wigner distribution in equation (5) as shown in figures 14 and 15 with the following results for the width:

	Prompt ϕ	$D_s^{\pm} \to \phi\pi^{\pm}$
LL	0.126 ± 0.003	1.55 ± 0.04
DD	2.54 ± 0.07	10.64 ± 0.14

Table 5: Width Γ [ps] of the time resolution for the reconstruction with TupleToolPropertime.

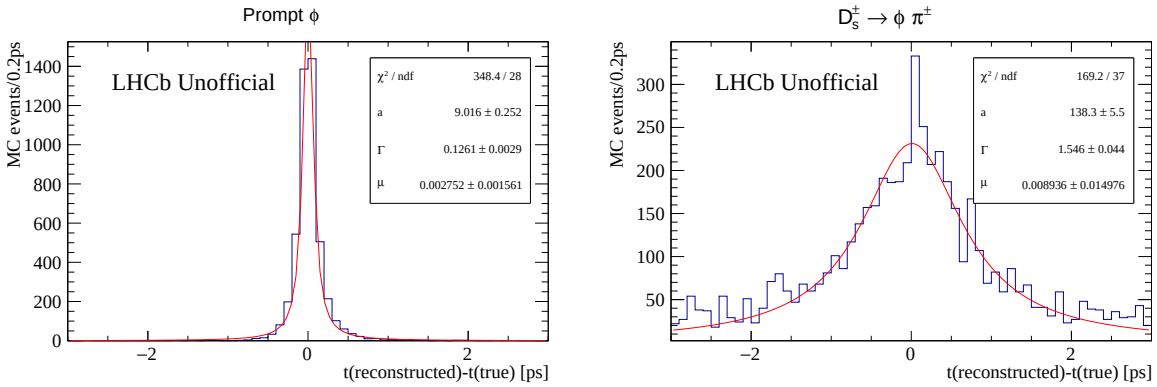

Figure 14: Resolution of LL kaon decay times t reconstructed via the DecayTreeFitter.

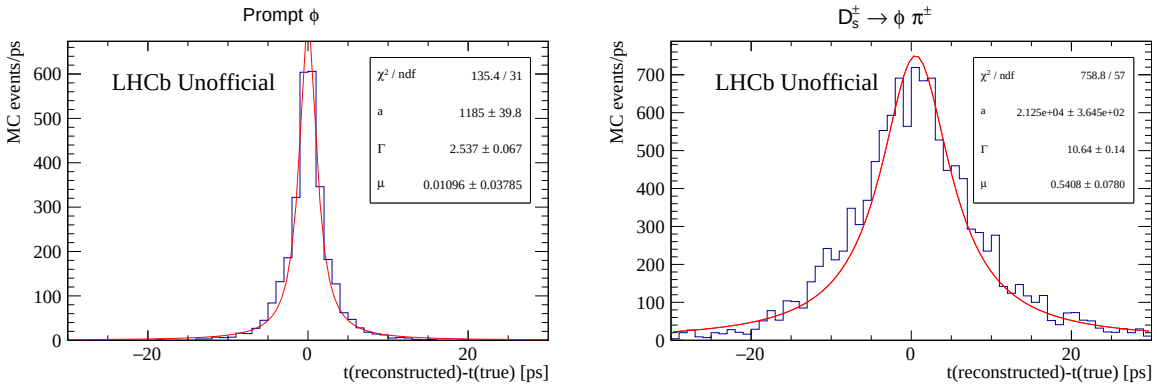

Figure 15: Resolution of DD kaon decay times t reconstructed via the DecayTreeFitter.

Additionally, the resolution of Δt has been determined by fitting the Breit Wigner distribution in equation (6) to the distribution of the residuals. Since in the Monte Carlo either both kaons are LL or one is LL and the other is DD, here, these two combinations have been studied. The plots illustrating the fit can be found in figures 16 and 17 and the widths in table 6.

	Prompt ϕ	$D_s^\pm \to \phi\pi^\pm$
LL and LL	0.24 ± 0.01	0.43 ± 0.01
LL and DD	2.47 ± 0.06	4.11 ± 0.05

Table 6: Width Γ [ps] of the decay time differences for kaons reconstructed using the TupleTool-Propertime.

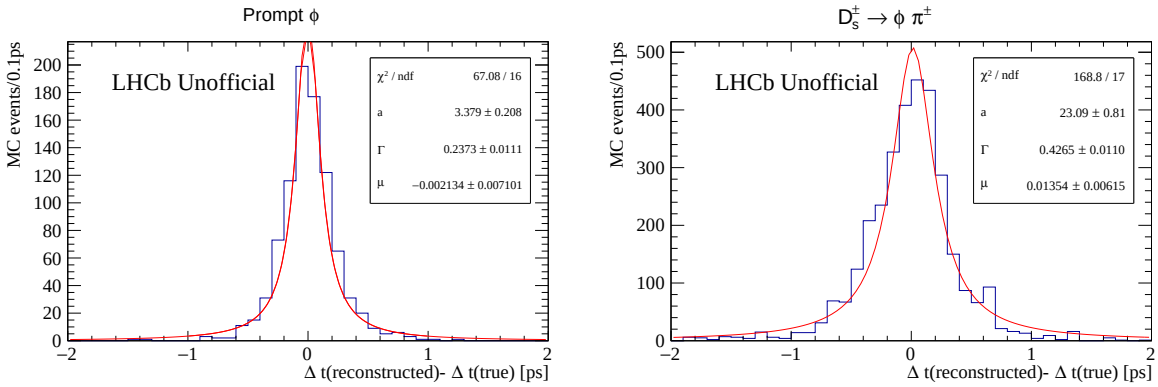

Figure 16: Resolution of Δt for LL kaons reconstructed using the TupleToolPropertime.

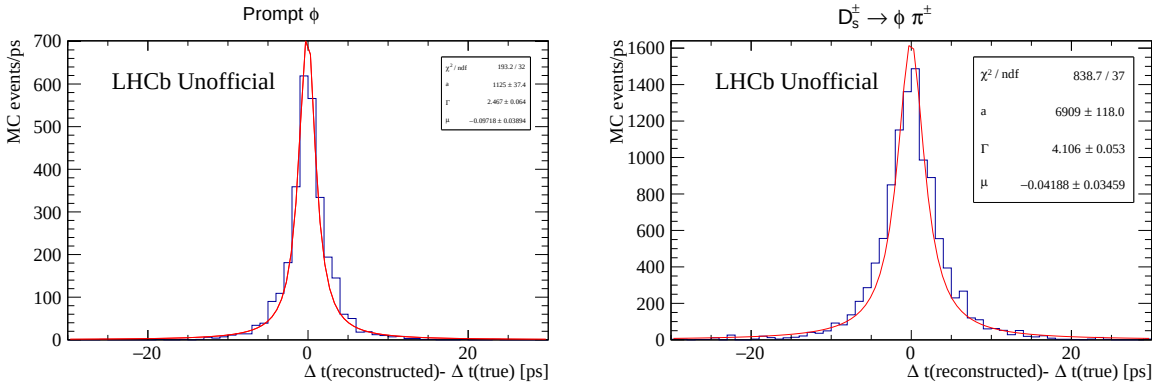

Figure 17: Resolution of Δt for LL and DD kaons reconstructed using the TupleToolPropertime.

For the $D_s^{\pm} \to \phi\pi^{\pm}$ case, the width of the resolution of the decay time difference is smaller than for the actual decay times since the ϕ lifetime is negligible and therefore the residuals of the kaon decay times are correlated through the common "vertex" $D_s^{\pm} \to K^0\overline{K}^0\pi^{\pm}$ as can be seen in figure 18.

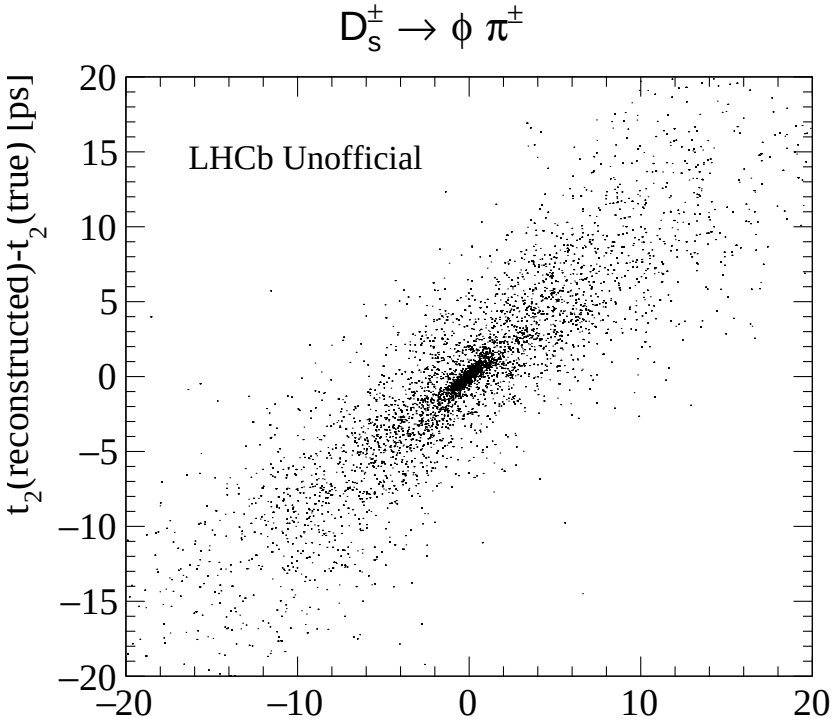

Figure 18: Correlation between the decay time residuals of both neutral kaons due to the common origin vertex.

6 Toy model for the prompt ϕ approach

Since the decay intensity of two prompt K_S is simply

$$I(t_1, t_2) \propto e^{-\Gamma_S t_1} e^{-\Gamma_S t_2}, \tag{7}$$

a toy study based on the assumption that all background consists of prompt K_S has been done using RooFit. To make the model more realistic, it includes an approximate transverse momentum distribution which is shown in figure 19.

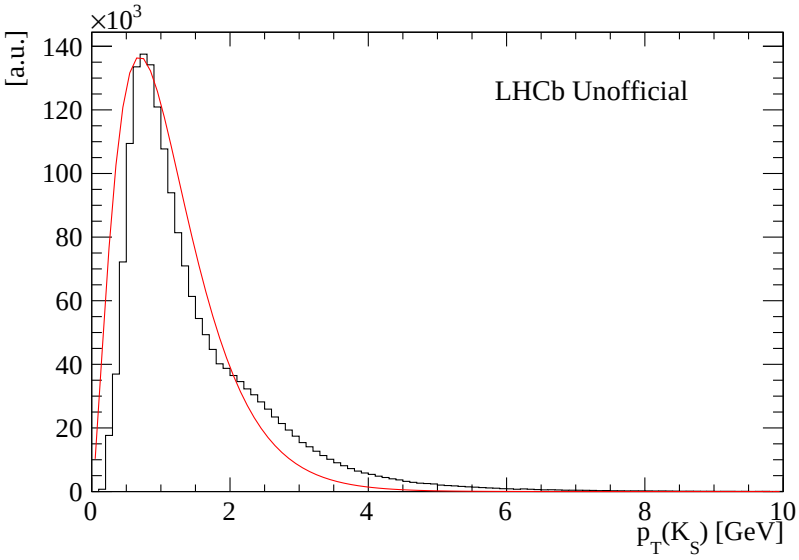

Figure 19: Transverse momentum of the kaons. The black line shows the distribution in 2012 data and the red line the approximation used in the model.

The approximative form used is

$$N(p_T(K_S)) \propto (p_T[MeV])^{1.52} \exp\left(-2.19 \cdot 10^{-3} p_T[MeV]\right) \tag{8}$$

It being part of the model is necessary in order to transfer the acceptance of events based on the transverse coordinates of the kaon decay vertices into the time domain that was studied. If for example both kaons decay inside the beampipe, that means that the x and y coordinate of their decay vertices have to be less than 7 mm.

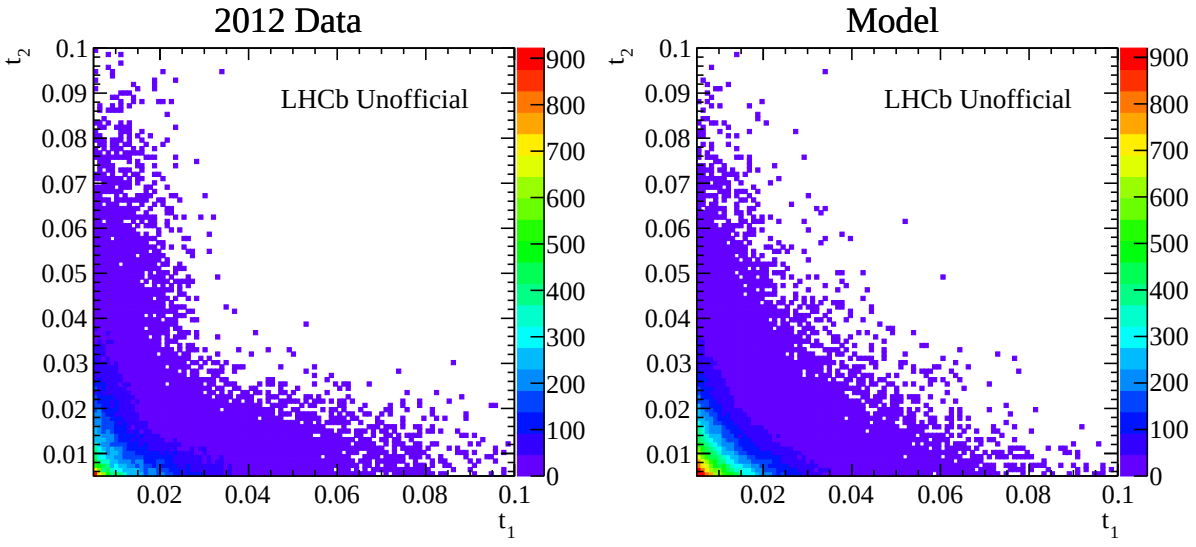

Figure 20: Comparison between the distribution in the lifetimes of the two kaons for 2012 data and the toy model studied.

The distribution of the decay times of the two kaons as given by the 2012 data and the model are displayed in figure 20
A toy dataset was built by combining this model of the prompt K_S with a similar one where the decay intensity of the kaons is replaced with the one given in equation (2) describing Standard Model background ($\zeta_{SL} = 0$). They were added with weights according to a signal to background ratio of $4 \cdot 10^{-4}$. This ratio is an optimistic estimate gained from the efficiency study in section 3.
Afterwards, the RooStats profile likelihood calculator was used to determine a 95% C.L. limit on ζ_{SL} for different luminosities based on this composite model. That was done by fitting equation (3) to the toy data set, leaving ζ_{SL} as a free parameter. The result is displayed in figure 21.
The predicted limits on ζ_{SL} go with the square root of the luminosity. The limits from the toy study have been fitted to a function with this behaviour. Based on this fit, it has been extrapolated that the necessary luminosity for being competitive with the KLOE limit $\zeta_{SL} = 0.098$ is $\int L\,dt \approx 275\,\mathrm{fb}^{-1}$. This is far beyond the amount of luminosity planned to be collected during run II and run III.

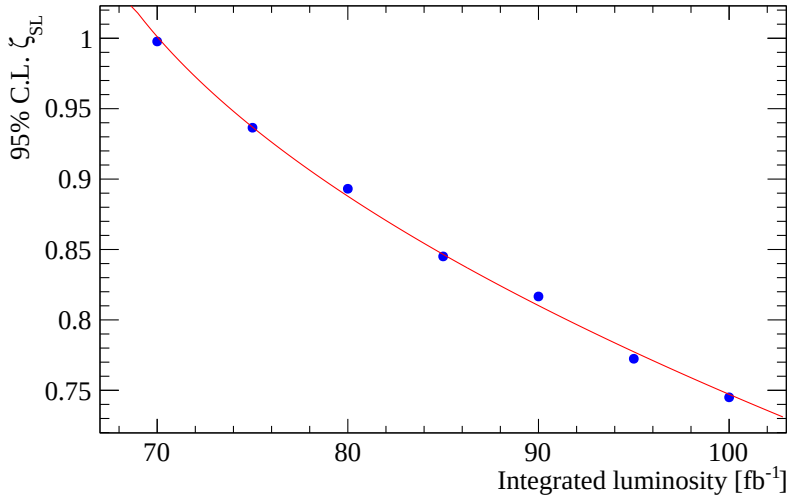

Figure 21: Predicted 95% C.L. limit on ζ_{SL} for the given luminosities.

7 Conclusion

The signal and background yields for the two approaches of ϕ selection have been calculated. The result suggests that the use of the topology $D_s^{\pm} \to \phi\pi^{\pm}$ does not offer significant improvement in the signal to background ratio.
The time resolution of the LHCb detector and the reconstruction algorithms commonly used by the collaboration have been studied in depth.
Finally, a toy study for the prompt ϕ approach has been conducted, resulting in the prediction that the luminosity needed at LHCb to reach the level of precision KLOE has

for the measurement of CPT invariance in $\phi \to K^0\overline{K}^0$ is in the order of $275\,\text{fb}^{-1}$.
It can be concluded that with the means currently available to LHCb, the study of CPT invariance in the given system does not seem feasible.

8 Acknowledgments

I would like to thank my supervisors Giulio Dujany and George Lafferty for giving me the opportunity to be a CERN summer student. Thank you for your support and counseling, it was great working with you! Thank you to Jonathan Harrison for providing a good part of the basis for my work and to Lorenzo Capriotti for helping me with my first steps using the Grid. I am very grateful to the entire LHCb group of the University of Manchester for welcoming me this summer.

References

[1] G. Lueders, *Proof of the TCP theorem*, Annals of Physics **2** (1957), no. 1 1 .

[2] J. Bernabeu *et al.*, *CPT and Quantum Mechanics Tests with Kaons*, in *Handbook on neutral kaon interferometry at a Φ-factory*, 2006. arXiv:hep-ph/0607322.

[3] Particle Data Group, K. A. Olive *et al.*, *Review of Particle Physics*, Chin. Phys. **C38** (2014) 090001.

[4] KLOE-2, I. Balwierz-Pytko, *Quantum Mechanics and CPT tests with neutral kaons at the KLOE experiment*, Acta Phys. Polon. Supp. **6** (2013), no. 4 1101, arXiv:1308.5813.

[5] F. Ambrosino *et al.*, *First observation of quantum interference in the process : A test of quantum mechanics and CPT symmetry*, Physics Letters B **642** (2006), no. 4 315 .

[6] LHCb Collaboration, R. Aaij *et al.*, *Measurement of the inclusive ϕ cross-section in pp collisions at $\sqrt{s} = 7$ TeV*, Phys. Lett. **B703** (2011) 267, arXiv:1107.3935.

[7] LHCb Collaboration, *Prompt charm production in pp collisions at $\sqrt{s} = 7$ TeV*, .

[8] LHCb Collaboration, *Track types*, https://twiki.cern.ch/twiki/bin/view/LHCb/LHCbTrackingStrategies#Track_types, 16.09.2015.

[9] W. D. Hulsbergen, *Decay chain fitting with a Kalman filter*, Nuclear Instruments and Methods in Physics Research A **552** (2005) 566, arXiv:physics/0503191.